



# Review of The Super Resolution Microsphere Optical Imaging Technique

Zainab A. Hrata<sup>\*1</sup>, Fatema H. Rajab<sup>2</sup>, Sorin L. Stanescu<sup>3</sup>

## Authors affiliations:

1\*) Dept. of Laser and Optoelectronics Engineering, Al-Nahrain University, Baghdad, Iraq. Laser and Optoelectronics Engineering Department, University of Technology. Baghdad, Iraq.  
[st.zainab.abdali.msc@ccd.nahrainuniv.edu.iq](mailto:st.zainab.abdali.msc@ccd.nahrainuniv.edu.iq)

2) Dept. of Laser and Optoelectronics Engineering, Al-Nahrain University, Baghdad, Iraq.  
[fatema.h.rajab@nahrainuniv.edu.iq](mailto:fatema.h.rajab@nahrainuniv.edu.iq)

3) LIG Nanowise Ltd, Unit 15 Williams House, Manchester Science Park, Manchester, M15 6SE, United Kingdom  
[sorin.stanescu@lig-nanowise.com](mailto:sorin.stanescu@lig-nanowise.com)

## Paper History:

Received: 12<sup>th</sup> Jan. 2024

Revised: 18<sup>th</sup> Jul. 2024

Accepted: 28<sup>th</sup> Jul. 2024

## Abstract

In this work we performed a review regarding the improvement of microscopical optical imaging assisted by using microspheres, focusing on the most recent technologies. We have been reviewed the utilizing of the superlens and nanojet concepts in order to understand the working principles of microspheres in terms of magnification and resolution improvement. Some researches about the parameters effecting on microsphere imaging technique have been presented including the effect of microsphere's material and size, the effect of immersion medium, and the plasmonic layer effect. Additionally, some applications that serve from this technique have been illustrated.

**Keywords:** Optical Microscope, Super Resolution, Photonic Nano Jet, Microsphere, Nano Imaging.

مراجعة لتقنية التصوير البصري بالكرات الدقيقة وفحص الدقة الفائقة

زينب عبد علي هراطة، فاطمة حامد رجب، سورين ل ستانسكو

الخلاصة:

في هذا العمل، قمنا بإجراء استعراض حول تحسين التصوير البصري المجهرى بواسطة استخدام الكرات الدقيقة، مركزين على أحدث التقنيات. لقد قمنا بمراجعة استخدام مفاهيم العدسة الفائقة والنانوجت بهدف فهم مبادئ عمل الكرات الدقيقة من حيث تحسين التكبير والدقة. تم تقديم بعض الأبحاث حول المتغيرات التي تؤثر في تقنية تصوير الكرة الدقيقة، بما في ذلك تأثير مواد وحجم الكرة الدقيقة، وتأثير وسط الغمر، وتأثير الطبقة البلازونية. بالإضافة إلى ذلك، تم توضيح بعض التطبيقات التي تستفيد من هذه التقنية.

## 1. Introduction

In the early years of microscopy, the main drawback in microscopy was the lenses/objective lens manufacturing issue. These issues was the blurring, the imperfection of the image formation and distortion due to the optical aberrations and impurities in the lenses. Despite this, across time, lenses fabrication quality was improved, for instance by the using of purer glass and enhancing achromatic lenses. this improvement, one was able to avoid color distortion and poor image resolution. After avoiding these two problems, and in order to increase the amount of light that been capture and improve the image, it was suggested to use compound lenses [1]. In 1932, one can mention a notable evolution in microscopy thanks to the invention of Frits Zernike. He invented the phase contrast microscopy, which enabled the observation of transparent specimens without the requirement of using fluorophores [2]. After six years, the electron microscope was developed by Ernst Ruska, a concept which is employing electrons (as opposed to light) to improve the resolution and

provide more details of the small features [3]. After many years, in 1981 Gerd Binnig and Heinrich, invented scanning tunneling microscope (STM);this microscope provides three dimension images of specimens at the atomic level by tunneling effect [4]. Then, the developments in imaging techniques have allowed the tracking of single proteins as they develop within cells, such as super-resolution fluorescence microscopy. This technique of imaging breaks the diffraction limit of light, increases magnification, enables the observation of smaller structures and finer details that might remain imperceptible using conventional microscopy methods [5]. However, there are several limitations of this technique, such as: the utilization of specific fluorophores which can be costly and may not be easily accessible for every application, repeating imaging and quenching processes can result in phototoxicity, it potentially causes damage or killing the cells, the variety of samples which can be imaged is limited, it is more complex than other techniques, demanding dedicated equipment and training [6]. Another imaging technique is by using an objective



lens of a microscope immersed in oil, i.e. known as oil immersion microscopy, this technique can provide an enhancement in the quality and resolution of the image by improving numerical aperture of the objective lens. However, the resolution provided remains inadequate for smaller structures. Since the goal of improving the imaging techniques is to enhance the ability to discriminate small structures, to break the light diffraction limit of light, and image subwavelength details while moving away from complex designs, it was necessary for the microsphere assisted microscopy to be demonstrated. Following these techniques, several efforts have been paid on analyzing and enhancing images of microsphere assisted optical microscopy. In 2011, Wang [7] achieved an optical resolution of 50 nm using a conventional optical microscope coupled with fused silica microspheres 4.74  $\mu\text{m}$  in diameter. This marked a record achievement in optical resolution with white light illumination. In 2014, Darafsheh, confirmed empirically that using the microspheres with traditional microscopes provides an image enhancement, including an improvement in image quality, higher contrast, and magnified images when compared with immersion objective lenses. By employing transparent microspheres on a sample using a standard microscope, will allow for overcoming the limitation of light diffraction, as illustrated in Figure 1. By collecting evanescent waves in the near field and converting them to propagating far field waves, allows a higher-resolution imaging of subwavelength details [8]. Recent work has illustrated that achieving super-resolution is possible by positioning the microsphere in a contactless arrangement with the object, thus enabling non-invasive acquisitions. Researchers had been proved that microspheres could be utilized in combination with different types of microscopes, *i.e.* in 2016, Wang used microspheres with coherence scanning interference microscopy and they obtained a lateral resolution of 60 nm in an immersion medium [9]. In 2017, a digital holographic microscope utilizing microspheres was developed for precise cell identification [10]. In 2022, Zang used a Leica DM2500M optical microscope assisted by microspheres for observing periodic nanoparticle samples [11]. While in 2023, Qi used microspheres on a reflected glass slide for dark-field microscopy [12]. Different types of microspheres can be used, such as silica glass, polystyrene and barium titanate. Also, microsphere-assisted-microscopy offers simplicity, label free imaging and it doesn't need any image post-processing.

In this paper, a review of microsphere assisted optical imaging is presented, focusing on its advantages, materials and applications.

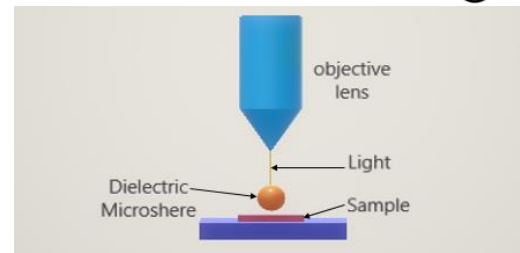


**Figure (1):** show a dielectric microsphere on a sample work as assisted lens with standard microscope.

## 2. Superlens

The superlens was firstly suggested and recommended by Sir John Pendry and known as the 'perfect lens, in 2000 in his paper entitled with 'Negative Refraction Makes a Perfect Lens'[13]. Pendry's proposal was based on the idea of using materials with negative refractive indices, which would allow for the manipulation of light in a way that was not possible with natural materials before. Superlens fabricated from unnatural material with a negative refractive index would allow the manipulation of the light in a way that was not possible in conventional lenses, as we know it is classified from natural material and has a positive refractive index[13]. This characteristic allows the superlens to enhance and restore the fine details beyond the diffraction limit object, unlike conventional lenses which cannot restore the information due to the loss of evanescent wave beyond the near field, as illustrated in schematic figure (2). The superlens resolving power exceeds the limited-resolution of conventional optical microscopes. The objective lens of a conventional microscope cannot discern sub-diffraction details of objects because it doesn't have the ability to capture the evanescent waves which carry the information about the features with dimensions beyond the diffraction limit, while superlenses can capture it and convert it to propagating waves which carry the diffraction limited details of the object. Also, superlenses can transmit features to the objective lens[13].

The superlens is classified in three types: optical near-field lens, far-filed superlens and hyperlens, as showed below.

### 2.1 Optical near-field superlens

The optical near-field superlens is manufactured from metallic structures vastly smaller than the light wavelength, which form the magnetic and electric fields and decrease p-polarized waves (Transverse Magnetic mode) [13]. It has been confirmed that silver is the preferred material for manufacturing these lenses due to its minimal loss factor within the optical range, making it the most common choice. However, it has two constraints: it is only effective in the near field when the gap between the object and the objective lens has a sub-wavelength dimension; the loss of evanescent waves in optical near field leads to low resolution [14].

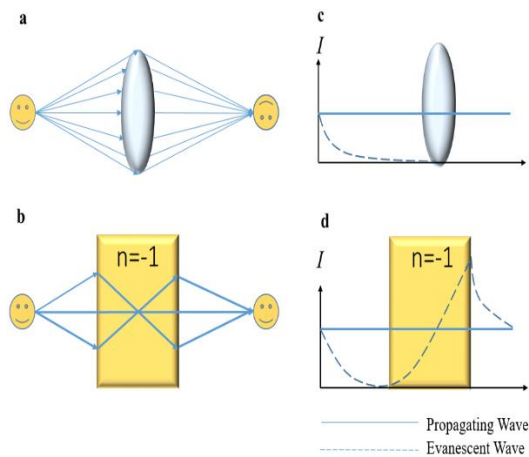


**Figure (2):** illustrates a conventional lens and a medium with a negative refractive index: (a) the transmission of waves through a conventional lens, (b) the absence of evanescent waves and the transmission of propagating waves, (c) the advancement of propagating waves in a medium with a negative refractive index, and (d) The advancement and restoration of both propagating and evanescent waves in a negative refractive index medium [15].

## 2.2 Optical far-field superlens

Unlike the optical near field, the optical far field superlens can overcome the distance limitation by coupling the evanescent wave with a propagating wave [16]. This far-field superlens provides an enhancement in evanescent waves and also it converts them into propagating waves [13]. This superlens is composed of silver-based subwavelength structures with additional nanoscale corrugations on its top surface [17], which serve in the enhancement of evanescent waves originating from fine details of objects and convert them into propagating waves so it can perceive the subwavelength features. An accurate transfer function is essential for the reconstruction process in order to generate images that surpass the diffraction limit. The feasibility of the proposal was evaluated using a silver FSL geometry operating at a wavelength of 377 nm [18], [19]. This setup enabled an image of nanowires with a width of 50 nm, which were spaced apart by a gap of 70 nm. A recently conducted study examined a tunable FSL that has the ability to operate at any wavelength within the visible spectrum [20]. This was achieved by substituting the silver slab with a stack of silver dielectric layers. Numerical computations demonstrated that a two-dimensional particle with a radius of 40 nm can be visualized with resolution that surpasses the diffraction limit by employing a multilayer FSL, generating sufficient evanescent wave enhancements through the excitation of surface plasmon [21]. Figure (3) demonstrates a schematic of far field super lens. Within this superlens technology, had been demonstrated an effectiveness in comparison with most near field superlens. In contrast, there are mainly two limitations: The distance between the sample and this superlens needs to be very small, and the image can be formed only in one dimension (1D) through the scattering of evanescent and propagating waves [21].

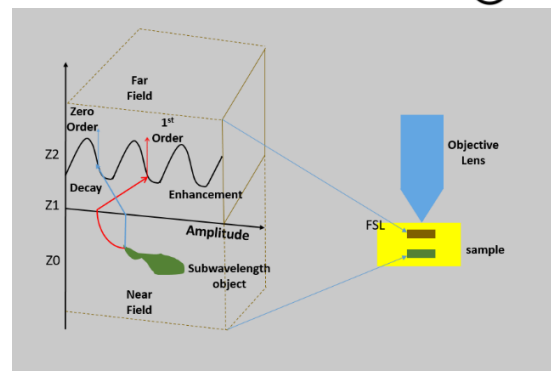


**Figure (3):** illustrates a far-field superlens. It can selectively enhance the evanescent waves emitted by the object and transform them into propagating waves. An FSL microscope can be created by placing an FSL component between the specimen and the objective lens of a standard microscope [22].

## 2.3 Hyperlens

As mentioned above with far field superlens, evanescent waves are initially improved by the plasmonic effect. Subsequently, they undergo conversion into propagating waves at the metamaterial's surface. However, it's important to note that the super resolution imaging effect is effective only in the last layer of the metamaterial within the near-field area [17]. This lens was manufactured of 16 curved periodic layers of 35nm thick silver and  $\text{Al}_2\text{O}_3$  on a substrate made of quartz. This structure allows far field hyperlens to magnify the sub-diffraction-limited object and deliver it to the far field area [16]. This procedure allows conventional microscopes to capture the image and increase its resolution compared to near-field and far-field superlens.

## 3. Photonic nanojet

When illuminating a dielectric spherical microsphere with a plane wave of a wavelength smaller than the sphere's radius, narrow and intense electromagnetic beams are formed in the shadow side of the sphere propagating in the surrounding medium. This beam is known in the literature as "PNJs" or "photonic nanojets" [23] and it was first mentioned by Chen in 2004 [15]. When incident light is concentrated directly on the distal surface or in its close proximity concerning the light source of the parent microelement, the interactions in the near-field between the boundary of microelement and the concentrated beam result in an interesting phenomenon: the creation of a highly localized electromagnetic beam. Extensive research efforts have been directed towards utilizing the characteristics of PNJs in both individual microelements and arrays, at different shapes. These efforts aim to explore a wide range of applications, including nano-photolithography, super-resolution imaging, as well as fluorescent and Raman spectroscopy, among others where it is required a localized intense beam of light [24]–[28].



When dielectric microspheres have sizes vastly smaller than the wavelength  $\lambda$  of illuminated light, the light will suffer scattering symmetrically in- forward and back-ward direction, this in respect with Rayleigh scattering phenomena [29], [30]. On the other hand, the focusing phenomena in large spheres (where the radius is significantly greater than the wavelength) can be effectively calculated using the formulas of classic optics [30]. On the other hand, when the sphere size's is comparable to the (wavelength  $\lambda$ ) of light, neither Rayleigh scattering phenomena, nor geometrical optics approximation can provide an accurate assessment of their interaction with light. In such cases, Mie's theory offers a comprehensive description of the interaction of light with microspheres particles of various sizes [30]. By applying the Mie theory, one can observe the field improvement achieved by dielectric spheres transformed from a Rayleigh scattering regime ( $r \ll \lambda$ ) with dipole structure to a mesoscale sphere with a jet-like formation ( $r$  approximately from 1 to  $30\lambda$ ). After observing the mesoscale sphere properties, it was illustrated that the specific characteristics such as the size and the refractive index of a microsphere (or in some cases a microcylinder) and the wavelength of light, when it is focused onto or close to the 'shadow-side' surface of the microsphere, then the phenomenon (the formation of photonic nanojets) is achieved. This happens due to the near-field interactions between the microsphere's boundary and the focused light beam.

In the microsphere assisted microscopy imaging field, studying the formation of PNJ's and their characteristics is very important for achieving super-resolution. PNJs have the potential to achieve lateral sizes smaller than the diffraction limit and they can propagate across multiple wavelengths with minimal divergence [15]. Thus, it is very important to study the key parameters of photonic nanojets (PNJs) including the beam's waist size, the decay length, the maximum beam intensity, and its location [31]. Figure 2 illustrates the schematic of a PNJ and its parameters. Its features can be controlled primarily by adjusting and altering factors such as the refractive index, size, and shape of the parent particle, as well as the refractive index of the surrounding medium. Furthermore, the characteristics of the nanojet are influenced by the properties of the incident light, such as the wavelength, intensity, phase distributions and the polarization state.

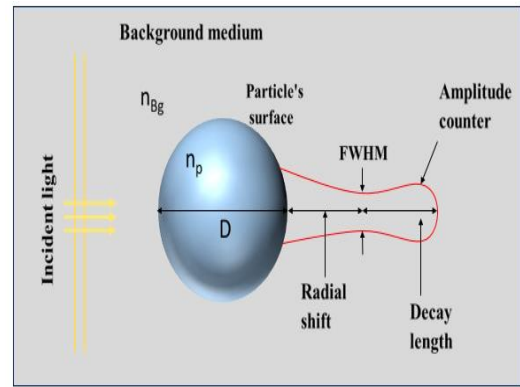


Figure (3): Schematic diagram of a PNJ and its parameters[23].

#### 4. Review of microsphere assisted optical imaging

This section reviews super resolution imaging techniques by using microsphere assisted conventional optical microscopy, as follows:

In 2013, Darafsheh [32] studied the super-resolution capability of high refractive index ( $n \sim 1.9-2.1$ ) barium titanate glass (BTG) microspheres immersed in isopropyl alcohol (IPA) with sizes ranging from several  $\mu\text{m}$  up to hundreds of  $\mu\text{m}$ . The study involved the use of an upright microscope with a microsphere placed in direct contact with a variety of semiconductor and metallic nanostructures or on a commercial Blue-Ray disk sample with nominal track pitch sizes of 300 nm comprised of 200 nm tracks separated by 100nm grooves. Their results indicated that by using 100 nm silver nanowires showed an improvement of approximately (1.7 times) in spatial resolution compared with standard optical microscopy. Furthermore, when 2-D nanoplasmonic arrays were utilized, the researchers demonstrated high resolution imaging by using small numerical aperture objective lenses. This property is desirable for achieving high-resolution-imaging when long distances between the objective lens and the sample are required. Moreover, in 2014, Darafsheh, [8] studied and compared imaging using a silica sphere ( $n=1.46$  with  $D=2-9 \mu\text{m}$ ) and BTG-SiO<sub>2</sub> sphere ( $n=2.1$  with  $D=15 \mu\text{m}$ ) immersed in liquid with traditional diffraction limited microscopy and solid immersion lens microscopy (SIL). They showed that using high refractive index liquid immersion microspheres results in superior image quality, higher resolution, and greater magnification compared with the images achieved by confocal and solid immersion lens (SIL) microscopy. They also showed that in comparison with microsphere-assisted imaging, in the air, provides superior quality imaging. They concluded that a high NA value and refractive index microsphere immersed in a liquid is useful for super-resolution imaging microscopy and they provide better quality with more contrast and higher magnification in comparison with liquid-immersion objectives. They also have clarified that microspheres immersed in liquids achieve higher numerical aperture values with larger working distance, which provides protection for the microscope's objective lens (against collision).



In 2015, Guo [33] studied the far field properties of microsphere imaging using high refractive index barium titanate glass (BTG) microsphere ( $n \sim 1.93$ ) and  $24 \mu\text{m}$  diameter separated by a SU-8 photoresist from the Blu-ray disk sample with distances ranging gradually from 0 to  $5.4 \mu\text{m}$ . The spheres were all fully immersed in ethanol for all the experiments. Their result showed that lateral magnification increased from 3.5x to 5.5x while the field of view (FOV) decreased from  $5.1$  to  $3.0 \mu\text{m}$ , as the distance ( $d$ ) increased between the microsphere and the object. They found out that by having a certain distance between the microsphere and the sample, the optical image can be optimized, improving the magnification, and capturing the diffraction-limited details of the object. Furthermore, they emphasized that the far-field imaging characteristics are related to the intensity profile of the electromagnetic field at various positions under the base of the microsphere.

In 2016, Hok [34] studied the effect of the diameter and refractive index of two types of microspheres- dry barium titanate and immersed polystyrene microspheres on the image resolution of two samples consisting of a blank blue-ray and a CPU. They used dry barium titanate glass microspheres with sizes ranging between  $20$  and  $220 \mu\text{m}$  and a refractive index of  $1.93$  and wet polystyrene microspheres with a diameter of  $30 \mu\text{m}$  and a refractive index of  $1.59$ . They also investigated the relationship between two factors: the focal position and the additional magnification by using empirical techniques and theoretical investigations. They concluded that high refractive index microspheres achieve virtual, super resolution images and they reported how the image formation and planes are affected by changing the microsphere's refractive index and diameter. They concluded that the resolution and the field of view (FOV) increased proportionally with the sphere's diameter and refractive index.

In 2017, Guo [35] studied the effect of a dielectric planar cavity (DCPP) on the optical images by combining it with silica microsphere lenses and compared the results from the point of view of image contrast and field of view without it. They found out that using an illustrated microsphere lens with a  $3.4 \mu\text{m}$  diameter combing a planar cavity with a thickness of about  $2.2 \text{mm}$ , the FOV was about  $2.4 \text{mm}$  and the magnification was about  $1.6$ . However, the  $1.5 \text{mm}$  FOV and the  $1.4$  magnification were achieved using a  $3.4 \text{mm}$  diameter microsphere lens without DCPP. They also found that image contrast could be enhanced by immersing the microspheres in ethanol. Therefore, they concluded that adding DCPP improved the FOV and the magnification of the image.

In 2018, Deng [36] studied the image features of a cascade microsphere lens and compared the results with a single lens microsphere structure. Then, they employed a PS microsphere array with  $960 \text{nm}$ -diameter low refractive index and a silica microsphere semi-immersed in ethanol with a diameter of  $3\text{--}6 \mu\text{m}$  and a refractive index of  $1.46$ . A Blu-ray disc was used as a sample and a Leica DM2500 M microscope equipped with a  $100\times/0.9\text{NA}$  objective lens were

employed for the experiments. Their results were based on a comparison between a single semi-immersed silica microsphere and three structures of cascade hexagonal PS microsphere. They revealed that the imaging magnification of the cascaded microsphere lens was approximately  $(1.4)$  times higher than that of the single silica microsphere semi-immersed in ethanol. They concluded that the imaging magnification could increase by using a cascade microsphere lens. Furthermore, they discovered that for the cascaded microsphere lens to function effectively, it is essential that the focal point to be positioned near the sample, and that the centers of the two microspheres should align along a line parallel to the direction of propagation.

In 2019, Perrin [37] used soda-lime-glass microspheres in air with diameters of  $25 \mu\text{m}$  and a refractive index of  $1.52$  to study the unconventional magnification. They used a white light with ( $\lambda_0 = 650\text{nm}$ ,  $\Delta \lambda = 400\text{nm}$ ) to illuminate the sample and also they used two wavelength filters (a cyan filter and a blue-line filter with  $\lambda_0 = 567\text{nm}$  and  $\Delta \lambda = 90\text{nm}$  and  $\lambda_0 = 445\text{nm}$  and  $\Delta \lambda = 11\text{nm}$ , respectively) to limit the spectral width of the light source. They studied the influence of both the axial image position and the microsphere's diameter on the magnification and the position-dependent magnification, respectively. They concluded that the size of the microsphere is inversely proportional to the increase in magnification, and it is directly related to the initial position of the axial field of view (FOV). Moreover, narrowing the spectral bandwidth of the illumination light source effectively decreases the magnification range.

In 2020, Yang [38] used a barium titanate glass (BTG-SiO<sub>2</sub>) sphere with  $\text{RI}=2.0$  and  $25 \mu\text{m}$  diameter immersed in ethanol with ( $\text{RI}=1.36$ ) as a dielectric microscope with the aim of studying the effect of the immersion depth of ethanol on barium titanate glass microspheres. They also studied the capability of coupling the evanescent waves to propagating waves and they had demonstrated it in their experimental section. A Blue-ray disk was used as a sample, illuminated by center wavelength  $540 \text{nm}$  from a Zeiss Axio Imager 2 microscope and the image was monitored with the gradual evaporation of ethanol with the aim of illustrating the effects of decreasing the immersion depth of ethanol (IDE) on the resolution of the image. They used the point-spread function (PSF) and a finite difference time-domain (FDTD) methods to quantify the resolution of the BTG microsphere-assisted microscope and measured the ability of microsphere of conversion evanescent waves to propagating waves, respectively. They concluded that the decreasing of IDE affected both the resolution and the position of optical image plan, which caused the decreasing in the resolution of microsphere assisted imaging microscope. Also, Liu [39] experimented microspheres with four different refractive indices for studying and selecting the proper type of microsphere for coupling them with optical tweezers with the aim of achieving super-resolution microsphere-assisted microscopy. They used SiO<sub>2</sub>, PS, melamine formaldehyde (MF) and BTG spheres with refractive index  $n \sim 1.46$ ,  $n \sim 1.59$ ,  $n \sim 1.68$  and  $n \sim 1.93$



respectively to achieve super-resolution for a silicon nanostructure grating (SNG) with 139 nm steps separated by a 139 nm gaps in an upright microscope illuminated by white light. Their results illustrated that both the polystyrene PS sphere and the MF with a 10- $\mu$ m diameter in deionized water ( $n \sim 1.33$ ) and moderate refractive index give the best trapping performance and maintain super resolution imaging. In addition, they demonstrated that a better image quality by the MF sphere is obtained compared to that by the PS sphere. Additionally, the PS sphere provides a 2x lateral magnification, while the MF sphere provides a 2.2x lateral magnification. They concluded that it is possible to achieve label-free super resolution imaging techniques by microsphere optical trapping manipulation.

In 2022, Wang [40] presented a procedure to enhance the performance of microscopy-assisted imaging by optimizing the refractive index of different immersion media. In this study, they employed polystyrene PS ( $n = 1.59$ ) and BTG microspheres ( $n = 1.90$ ) with 10  $\mu$ m diameter for both types of spheres and the immersion mediums used included water, spin-on-glass (SOG), SU-8 photoresist and S1805 photoresist with refractive indices of  $n = 1.33$ ,  $n = 1.46$ ,  $n = 1.60$ ,  $n = 1.65$ , respectively. Also, they utilized various samples, including Blu-ray discs, 250 and 200 nm silica nanoparticle arrays and digital video discs (DVDs) as samples. They used two software for modeling: COMSOL to simulate the electric field intensity distribution and ZEMAX to simulate spherical aberrations and distortions of microspheres particle. The experimental result revealed that the distortions of images is smaller when PS microsphere are used compared to fully immersion of BTG with the same immersion medium. In addition, a semi-immersed PS microsphere in SU-8 photoresist which produced the smallest image distortion, narrowest waist, the strongest peak intensity and the shortest "focal" length ( $L$ ) from the center of the sphere to the point of maximum intensity for notice the last three parameter refers to photonic nanojet. They concluded that higher contrast and resolution could be achieved by employing a semi-immersed PS microsphere in SU-8 photoresist, which has superb focusing properties. Moreover, the clearest images were obtained by adjusting the working distance between the objective lens and the microsphere.

In 2023, Qi [12] proposed a method to improve the contrast and resolution of imaging low-contrast samples based on the reflection and scattering of light. PS nanoparticles  $d = 150 - 300$  nm and a silver coated substrate were used for imaging 250 nm hexagonally closed packed polystyrene nano particles via dark field microscopy. The demonstrated that the contrast had been improved, and the resolution was increased by 4.9 times when compared with the same object positioned on a glass slide and imaged by dark field mode microscopy. They concluded that without the reflective substrate and microsphere, the object cannot be observed in dark field. Table 1 states important information regarding the literature review showing previously work and giving indication about the author, year of study, used material (type, size),

medium, object and on the image magnification. Despite previously published works, the microsphere assisted optical imaging theory still requires deep studying, analyzing and improving.

## 5. Applications of microsphere assisted optical imaging

Microspheres enable high-super-resolution imaging and contribute to overcoming the limitations imposed by diffraction in various types of microscopes, as explained below:

**White light microscope:** Because of the diffraction limit, it is hard to image finer details with sub-wavelength features. On the other hand, by using microspheres in different media on a sample it will be effective for providing high-resolution image by using halogen lamp with a central wavelength of 600 nm. Different studies illustrated that high resolution could be achieved using white light microscopy with fused silica microspheres in air [41], semi-immersing liquid of ethanol [42], microscope-immersion oil [43] and BTG ( $\text{BaTiO}_3$ ) microsphere-immersion in isopropyl alcohol [44]. Also, there has are studies where it is shown that super-resolution imaging is achievable by using microspheres embedded in a transparent solidified film [44].

**Scanning laser confocal microscopy (SLCM)** [45] using 5  $\mu$ m diameter fused silica to form image of an array of gold quintuplet nanodots coated on a glass substrate with resolution 25 nm were also performed. In this resulted images, the resolved nanodots were in direct contact with the microsphere., The nanodots not in contact with the microspheres appeared distorted and blurred. The experimental outcome suggests that the MSLCM can effectively resolve individual objects with spatial separations smaller than the used wavelength of light used for illumination.

**Coherent anti-Stokes Raman Scattering microscopy** [46], [47] used with  $\text{SiO}_2$  microspheres on an organic azo-dye film consisting of stripes 200 nm wide with 100 nanometer-wide grooves between them, the grooves having a depth of 20 nanometers. The E-CARS itself was unable to observe sub-diffraction pattern that the resultant image magnification was up to 5X larger, with achieved far-field lateral resolution of at least  $\lambda p/4$ , where  $\lambda p$  is pumping laser wavelength, which in their case it was 796nm. Fluorescent microscopy [48] could not resolve 100 nm-diameter polystyrene fluorescent particles on a glass substrate. However, by incorporating a 60  $\mu$ m diameter barium titanate microsphere the sample was resolved and the magnification calculated was 5.4 times, allowing the visualization of a 1  $\mu$ m-diameter particle. This implies that the technique has the potential to visualize features much smaller than the diffraction limit.

**Photoacoustic microscopy** [49], [50] Photoacoustic imaging (PAI) is an emerging hybrid imaging technique with both preclinical and clinical applications. It involves irradiating the biological tissue with nanosecond laser pulses, causing the tissue to absorb light, resulting in a local temperature increase and the emission of pressure waves in the form of sound waves. Ultrasound detectors collect these photoacoustic signals to create images of the internal



structure and function of biological tissue. However, the potential of achieving super-resolution in (photoacoustic imaging PAI) using a microsphere approach, particularly through the use of photonic nanojets and break the diffraction limit was very important in providing the way for many applications, including non-invasive medical imaging, the study of cellular and subcellular structures, and potentially revolutionizing the way we visualize and understand biological tissues. This can contribute to early disease detection, precise diagnostics, and advanced research in various fields.

## 6. Conclusions

A review about improvement of imaging technique by an optical microscope was illustrated, focusing on

microsphere-assisted-microscopy. The concept of photonic nanojet and superlens had been detailed and utilized to understanding the principle's work of microspheres. Parameters affecting on high-resolution imaging technique using microspheres have been discussed. It can be concluded that the size, material of microsphere and the immersion environment affects the image resolution and magnification. Additionally, some applications, such as medical and biological, which serve from this technique, have been illustrated. From this review, it can be concluded that despite previously published works; the microsphere assisted optical imaging theory and principle work as well as their applications still require deep studying, analyzing and improving.

**Table 1:** Review of microsphere assisted optical imaging

Author	Years	Sphere type	Sphere size	Medium	Object	Magnification
Darafsheh [32]	2013	BTG	Several to hundred um	IPA	Blue-ray disk	3.6x
Darafsheh [8]	2014	SiO <sub>2</sub>	2-9 um	IPA	Blue-ray disk	5x
		BTG	15 um			
Guo [33]	2015	BTG	24 um	Ethanol	Blue-ray disk	5.5x
Hok [34]	2016	BTG	20-220um	Air	Blue-ray disk & CPU	6.44x
		PS	30um	Wet it in deionized water		6.92x
Guo [35]	2017	SiO <sub>2</sub>	3.4um	air	Blue-ray disk	1.6x
Deng [36]	2018	PS	960 nm arrays	ethanol	Blue-ray disk	1.4x
		Sio <sub>2</sub>	3-6 um			2x
Perrin [37]	2019	Soda lime glass	25 um	air	Grating with 400nm period	8x
Yang [38]	2020	BTG	25 um	ethanol	Blue-ray disk	-----
Liu [39]	2020	PS	10um	Deionized water	Silicon nanostructure grating	2x
		MF				2.2x
Wang [40]	2022	BTG Ps	10um	Water	Blue-ray DVDs Silica nanoparticles array	-----
				SOG		
				Su-8 resist		
				S180s resist		
Qi [12]	2023	PS	150-300 nm	air	hexagonally close packed polystyrene nano particles	-----

## 7. References

[1] "The Microscope | Science Museum." Accessed: Nov. 22, 2023. [Online]. Available: <https://www.sciencemuseum.org.uk/objects-and-stories/medicine/microscope>

[2] 1888-1966 Frits Zernike, "first," p. 282, 2008.

[3] E. Ruska, "Electron Microscope and of Electron Microscopy," *Les Prix Nobel 1986 Nobel Prize. Present. Biogr. Lect.*, p. 58, 1987.

[4] G. Binnig and H. Rohrer, "Scanning Tunneling Microscopy—from Birth to Adolescence (Nobel Lecture)," *Angew. Chemie Int. Ed. English*, vol. 26, no. 7, pp. 606–614, 1987, doi: 10.1002/anie.198706061.

[5] B. Huang, M. Bates, and X. Zhuang, "Super-resolution fluorescence microscopy," *Annu. Rev. Biochem.*, vol. 78, pp. 993–1016, 2009, doi: 10.1146/annurev.biochem.77.061906.092014.

[6] "Beyond the Limit: The World of Super-Resolution Microscopy | Labcompare.com." Accessed: Nov. 22, 2023. [Online]. Available: <https://www.labcompare.com/10-Featured-Articles/342799-Beyond-the-Limit-The-World-of-Super-Resolution-Microscopy/>

[7] Z. Wang, Guo, L. Li, B. Luk'Yanchuk, Khan, Liu, Chen, Hong "Optical virtual imaging at 50 nm lateral resolution with a white-light nanoscope," *Nat. Commun.*, vol. 2, no. 1, pp. 1–6, 2011, doi: 10.1038/ncomms1211.

[8] A. Darafsheh, N. I. Limberopoulos, J. S. Derov, D.

E. Walker, and V. N. Astratov, "Advantages of microsphere-assisted super-resolution imaging technique over solid immersion lens and confocal microscopies," *Appl. Phys. Lett.*, vol. 104, no. 6, 2014, doi: 10.1063/1.4864760.

[9] F. Wang, Liu, Yu, Liu, Yu, Wang, and Li, "Three-dimensional super-resolution morphology by near-field assisted white-light interferometry," *Sci. Rep.*, vol. 6, no. 1, p. 24703, 2016.

[10] P. C. Montgomery and D. Montaner, "Deep submicron 3D surface metrology for 300 mm wafer characterization using UV coherence microscopy," *Microelectron. Eng.*, vol. 45, no. 2–3, pp. 291–297, 1999.

[11] J. Zang, Y. Pei, S. Yang, Y. Cao, and Y. H. Ye, "Microsphere-Assisted Imaging of Periodic and Non-Periodic Structures," *IEEE Photonics Technol. Lett.*, vol. 34, no. 6, pp. 341–344, 2022, doi: 10.1109/LPT.2022.3155742.

[12] M. Qi, M. Zhang, D. Wang, S. Yang, Y. Cao, and Y. H. Ye, "Reflective Substrate-Enhanced Microsphere-Assisted Dark-Field Microscopy," *IEEE Photonics Technol. Lett.*, vol. 35, no. 21, pp. 1159–1162, 2023, doi: 10.1109/LPT.2023.3306913.

[13] J. B. Pendry, "Negative refraction makes a perfect lens," *Phys. Rev. Lett.*, vol. 85, no. 18, p. 3966, 2000.

[14] W. Cai and V. M. Shalaev, *Optical metamaterials*, vol. 10, no. 6011. Springer, 2010.

[15] Z. Chen, A. Taflove, and V. Backman, "Photonic



- nanojet enhancement of backscattering of light by nanoparticles: a potential novel visible-light ultramicroscopy technique,” *Opt. Express*, vol. 12, no. 7, pp. 1214–1220, 2004.
- [16] S. Lee, “Super-resolution Optical Imaging Using Microsphere Nanoscopy The University of Manchester,” 2013.
- [17] X. Zhang and Z. Liu, “Superlenses to overcome the diffraction limit,” *Nat. Mater.*, vol. 7, no. 6, pp. 435–441, 2008.
- [18] Z. Liu, S Durant, H Lee, Y Pikus, N Fang, Y Xiong, C Sun, X Zhang, “Far-field optical superlens,” *Nano Lett.*, vol. 7, no. 2, pp. 403–408, 2007, doi: 10.1021/nl062635n.
- [19] Z. Liu, S Durant, H Lee, Y Pikus, Y Xiong, C Sun, X Zhang, “Experimental studies of far-field superlens for sub-diffractive optical imaging,” *Opt. Express*, vol. 15, no. 11, pp. 6947–6954, 2007.
- [20] S. Dolnicar, Y Xiong, Z Liu, S Durant, H Lee, C Sun, X Zhang, “Tuning the far-field superlens: from UV to visible,” *Annals of Tourism Research*, vol. 3, no. 1, pp. 1–2, 2015. [Online]. Available: <http://www.sciencedirect.com/science/article/pii/S0160738315000444>
- [21] Y. Xiong, Z. Liu, C. Sun, and X. Zhang, “Two-dimensional imaging by far-field superlens at visible wavelengths,” *Nano Lett.*, vol. 7, no. 11, pp. 3360–3365, 2007.
- [22] X. Zhang and Z. Liu, “Superlenses to overcome the diffraction limit,” *Nat. Mater.*, vol. 7, no. 6, pp. 435–441, 2008, doi: 10.1038/nmat2141.
- [23] A. Darafsheh, “Photonic nanojets and their applications,” *J Phys Photonics*, vol. 3, no. 2, 2021, doi: 10.1088/2515-7647/abdb05.
- [24] A. Heifetz, S.-C. Kong, A. V Sahakian, A. Taflove, and V. Backman, “Photonic nanojets,” *J. Comput. Theor. Nanosci.*, vol. 6, no. 9, pp. 1979–1992, 2009.
- [25] A. Darafsheh, “Optical super-resolution and periodical focusing effects by dielectric microspheres.” The University of North Carolina at Charlotte, 2013.
- [26] B. S. Luk’yanchuk, R. Paniagua-Domínguez, I. Minin, O. Minin, and Z. Wang, “Refractive index less than two: photonic nanojets yesterday, today and tomorrow,” *Opt. Mater. Express*, vol. 7, no. 6, pp. 1820–1847, 2017.
- [27] J. Zhu and L. L. Goddard, “All-dielectric concentration of electromagnetic fields at the nanoscale: the role of photonic nanojets,” *Nanoscale Adv.*, vol. 1, no. 12, pp. 4615–4643, 2019.
- [28] X. A. Zhang, I.-T. Chen, and C.-H. Chang, “Recent progress in near-field nanolithography using light interactions with colloidal particles: from nanospheres to three-dimensional nanostructures,” *Nanotechnology*, vol. 30, no. 35, p. 352002, 2019.
- [29] J. W. Strutt, “LVIII. On the scattering of light by small particles,” *London, Edinburgh, Dublin Philos. Mag. J. Sci.*, vol. 41, no. 275, pp. 447–454, 1871.
- [30] H. C. Hulst and H. C. van de Hulst, *Light scattering by small particles*. Courier Corporation, 1981.
- [31] A. V Itagi and W. A. Challenor, “Optics of photonic nanojets,” *JOSA A*, vol. 22, no. 12, pp. 2847–2858, 2005.
- [32] A. Darafsheh, Limberopoulos, Derov, Walker Jr., Durska, Krizhanovskii, Whittaker, and Astratov “Optical microscopy with super-resolution by liquid-immersed high-index microspheres,” *Nanoscale Imaging, Sensing, Actuation Biomed. Appl. X*, vol. 8594, no. February 2013, p. 85940C, 2013, doi: 10.1117/12.2005896.
- [33] M. Guo, Y.-H. Ye, J. Hou, and B. Du, “Experimental far-field imaging properties of high refractive index microsphere lens,” *Photonics Res.*, vol. 3, no. 6, p. 339, 2015, doi: 10.1364/prj.3.000339.
- [34] H. Sum, Lai, Wang, Li, Jia, Liu, and Jung Li, “Super-Resolution Real Imaging in Microsphere-Assisted Microscopy,” pp. 1–17, 2016, doi: 10.1371/journal.pone.0165194.
- [35] M. Guo, Y. Ye, J. Hou, B. Du, and T. Wang, “Imaging of sub-surface nanostructures by dielectric planar cavity coupled microsphere lens,” *Opt. Commun.*, vol. 383, pp. 153–158, 2017, doi: 10.1016/j.optcom.2016.09.002.
- [36] Y. Deng, Yang, Xia, Cao, Jianguo Wang, Fengge Wang, and Ye, “Super-resolution imaging properties of cascaded microsphere lenses,” *Appl. Opt.*, vol. 57, no. 20, p. 5578, 2018, doi: 10.1364/ao.57.005578.
- [37] S. Perrin, H. Li, S. Lecler, and P. Montgomery, “Unconventional magnification behaviour in microsphere-assisted microscopy,” *Opt. Laser Technol.*, vol. 114, no. January, pp. 40–43, 2019, doi: 10.1016/j.optlastec.2019.01.030.
- [38] S. Yang, Y. H. Ye, Q. Shi, and J. Zhang, “Converting Evanescent Waves into Propagating Waves: The Super-Resolution Mechanism in Microsphere-Assisted Microscopy,” *J. Phys. Chem. C*, vol. 124, no. 47, pp. 25951–25956, 2020, doi: 10.1021/acs.jpcc.0c07067.
- [39] X. Liu, S. Hu, Y. Tang, Z. Xie, J. Liu, and Y. He, “Selecting a proper microsphere to combine optical trapping with microsphere-assisted microscopy,” *Appl. Sci.*, vol. 10, no. 9, 2020, doi: 10.3390/app10093127.
- [40] J. Wang, S. Yang, X. Wang, and Y. Cao, “Improved performance in microsphere-assisted 2D and 3D imaging by polystyrene microspheres semi-immersed in SU-8 resist,” *AIP Adv.*, vol. 12, no. 3, 2022, doi: 10.1063/5.0075275.
- [41] Z. Wang, W Guo, L Li, B Luk’Yanchuk, A Khan, Z Liu, Z Chen, M Hong, “Optical virtual imaging at 50 nm lateral resolution with a white-light nanoscope,” *Nat. Commun.*, vol. 2, no. 1, p. 218, 2011.
- [42] X. Hao, C. Kuang, X. Liu, H. Zhang, and Y. Li, “Microsphere based microscope with optical super-resolution capability,” *Appl. Phys. Lett.*, vol. 99, no. 20, 2011.
- [43] X. Hao, C. Kuang, Y. Li, X. Liu, Y. Ku, and Y. Jiang, “Hydrophilic microsphere based mesoscopic-lens microscope (MMM),” *Opt. Commun.*, vol. 285, no. 20, pp. 4130–4133, 2012.
- [44] A. Darafsheh, G. F. Walsh, L. Dal Negro, and V. N. Astratov, “Optical super-resolution by high-index liquid-immersed microspheres,” *Appl. Phys. Lett.*, vol. 101, no. 14, 2012.
- [45] Y. Yan, L. Li, C. Feng, W. Guo, S. Lee, and M. Hong, “Microsphere-coupled scanning laser confocal nanoscope for sub-diffraction-limited imaging at 25 nm lateral resolution in the visible spectrum,” *ACS Nano*, vol. 8, no. 2, pp. 1809–1816, 2014.
- [46] P. K. Upputuri, Z. Wu, L. Gong, C. K. Ong, and H. Wang, “Super-resolution coherent anti-Stokes Raman scattering microscopy with photonic nanojets,” *Opt. Express*, vol. 22, no. 11, pp. 12890–12899, 2014.
- [47] X. Huang, XN He, W Xiong, Y Gao, LJ Jiang, L Liu, YS Zhou, L Jiang, JF Silvain, YF Lu, “Contrast enhancement using silica microspheres in coherent anti-Stokes Raman spectroscopic imaging,” *Opt. Express*, vol. 22, no. 3, pp. 2889–2896, 2014.
- [48] H. Yang, N. Moullan, J. Auwerx, and M. A. M. Gijs, “Super-resolution biological microscopy using virtual imaging by a microsphere nanoscope,” *Small*, vol. 10, no. 9, pp. 1712–1718, 2014.
- [49] P. K. Upputuri, M. Krisnan, and M. Pramanik, “Microsphere enabled subdiffraction-limited optical-resolution photoacoustic microscopy: a simulation study,” *J. Biomed. Opt.*, vol. 22, no. 4, p. 45001, 2017.
- [50] P. K. Upputuri, Z.-B. Wen, Z. Wu, and M. Pramanik, “Super-resolution photoacoustic microscopy using photonic nanojets: a simulation study,” *J. Biomed. Opt.*, vol. 19, no. 11, p. 116003, 2014.